agronomy

Article

Crop Residue Removal Effects on Soil Erosion and Phosphorus Loss in Purple Soils Region, Southwestern China

Yuxin He [1,†], Kaicheng Yang [1,†], Wenhua Zhuang [1,*], Chao Liu [1], Longguo Li [1], Chi Zhang [1] and Mingming Li [2]

1 State Key Laboratory of Hydraulics and Mountain River Engineering, Sichuan University, Chengdu 610000, China
2 Institute of Mountain Hazards and Environment, Chinese Academy of Sciences, Chengdu 610041, China
* Correspondence: zhuangwenh@scu.edu.cn
† These authors contributed equally to this work.

Abstract: Background: Purple soil has a fragile structure and is highly vulnerable to soil erosion and phosphorus (P) loss risks. Despite this, the region is endowed with abundant crop residue resources. To ensure sustainable agricultural development in this area, we conducted a study to investigate the impact of crop residue removal on soil aggregate structure, soil erosion, and the risk of *P* loss. Methods: We conducted a three-year on-farm experiment and analyzed various soil parameters. These parameters include mean weight diameter (*MWD*), geometric mean diameter (*GMD*), soil aggregates with a diameter greater than 0.25 mm ($R_{>0.25mm}$), saturated hydraulic conductivity, soil erosion estimated by RUSLE 2, total soil phosphorus (*TP*) concentration, geometric mean concentration of *TP* (*GMC*), and geometric mean concentration of *TP* adjusted for aggregate size (GMC_d). Results: Retaining all crop residue can significantly improve soil saturated hydraulic conductivity, which was 2.56 times higher than the complete removal treatment. After three years of experimentation, compared to four months, the 50% residue removal treatment increased the GMC_d by 32.7%, while the 0% removal treatment increased the GMC_d by 16.6%. Both improvements were higher than the complete removal treatment. Partial or complete removal of the crop residue can reduce the soil aggregate stability and increase the risk of soil erosion and *P* loss. Conclusions: The *GMC* and GMC_d have the potential to serve as indicators for evaluating soil *P* loss risk. Removing crop residues can cause the degradation of the structure of purple soil aggregates, thus resulting in increased soil erosion and *P* loss. It is not recommended to remove crop residues in the purple soil region to ensure sustainable agricultural development.

Keywords: purple soil; crop residue removal; soil erosion; phosphorus loss

check for updates

Citation: He, Y.; Yang, K.; Zhuang, W.; Liu, C.; Li, L.; Zhang, C.; Li, M. Crop Residue Removal Effects on Soil Erosion and Phosphorus Loss in Purple Soils Region, Southwestern China. *Agronomy* **2023**, *13*, 1137. https://doi.org/10.3390/agronomy13041137

Academic Editors: Massimo Fagnano and Xiaobing Liu

Received: 28 February 2023
Revised: 4 April 2023
Accepted: 13 April 2023
Published: 17 April 2023

1. Introduction

Sichuan province is a significant grain production base in southwestern China that relies on its unique purple soil for the cultivation of its abundant agricultural products. The purple soil is rich in mineral nutrients [1], but the local mountainous and hilly topography and the scattered cultivated land on small steep slopes create poor aggregate structures and erosion resistance of the purple soil [2,3]. The purple soil layer is only about 50 *cm* thick [4], and the uneven rainfall in Sichuan mostly occurs during summer [5], thereby leadings to soil colloidal particles easily dispersing and migrating [3].

The high crop yield in Sichuan generates a significant amount of by-products, including straw, that has earned Sichuan the reputation of being a bioethanol base [6]. From 2007 to 2016, the annual average output of straw exceeded 15 million tons, which accounted for about 12% of the national output [6]. However, crop residue is frequently removed from farmland as a source of bioenergy, livestock feed, and other purposes, thereby resulting in significant nutrients lost from farmland [7], which leads to artificial fertilizer overuse and severe environmental impacts. Both crop residue removal and fertilizer overuse have caused soil degradation, including the loss of soil organic matter, low soil fertility, and inefficient nutrient use, which lead to low yield and agricultural non-point source pollution [8]. The excessive removal of straw from farmland has greatly depleted soil nutrients and had led to a reduction in the long-term production capacity of soil resources by disrupting the ecosystem mass balance [9–11]. The residue removal above a certain threshold leads to a decrease in soil quality [12], and the magnitude of this threshold is influenced by climate and soil conditions, thereby making the effect of removal on soil productivity specific to each site [13]. The achievement of sustainable agriculture in purple soil cultivated areas is limited by crop residue removal, thereby making it necessary to explore the threshold for crop residue removal in these regions.

Soil degradation is a critical issue that can result in reduced soil fertility, crop yields, and nutrient storage capacity, which leads to increased nutrient loss from farmland and the eutrophication of downstream water bodies [14] and poses a significant threat to environmental water quality and security [15]. In an effort to compensate for nutrient loss, local producers [7] apply more synthetic fertilizers, which results in a nutrient surplus, particularly of phosphorus (*P*), in the soil [16], which increases the risk of soil *P* loss and agricultural non-point source pollution [7,16,17], particularly in purple soil farmlands in southwestern China. *P* can enter water bodies from farmlands through surface runoff and soil erosion caused by rainfall and runoff [18]. The *P* loss from agricultural land with runoff can be classified into two forms—dissolved phosphorus (DP) and sediment extractable phosphorus (SEP)—with research indicating that the *P* loss in surface runoff in the form of SEP accounts for 88.3% to 92.8% of the total phosphorus (*TP*) loss [19–23]. However, previous studies using simulated rainfall experiments can convert some SEP into DP during the sampling process in runoff [20,21,24,25]. Leaching experiments, which estimate the effect of straw removal on soil *P* loss risk by measuring the *P* content of the leachate [26], can minimize the dissolution of SEP during testing. In this study, we utilized the wet sieve method and the leaching experiment to measure the dissolved and sedimented *P*, respectively. Additionally, the RUSLE 2 model was employed to simulate soil erosion and to evaluate the effect of different crop residue removal rates on the risk of purple soil erosion.

Factors affecting the impact of crop residue removal on soil *P* loss risk include soil physical structure, chemical composition, treatment duration, and removal rate [27]. Despite previous studies examining soil aggregate structure and chemical components, little research has been conducted on the elemental content of different-sized soil aggregates [28], thereby making it difficult to determine an optimal removal rate strategy [29,30]. To accurately assess *P* distribution and soil *P* loss risk, the distribution of *TP* in soil aggregates must be considered, as *TP* distribution is non-uniform, and small aggregates are more susceptible to erosion. When considering the different effects of the *TP* content of the aggregates in different sizes on the risk of soil *P* loss, it is particularly important to combine the expression of the size and the *TP* concentration of corresponding aggregates. In our study, we calculated the geometric mean concentration (*GMC*) and geometric mean concentration modified by particle size diameter (GMC_d) by integrating the size with the *TP* concentration of the corresponding aggregates in the calculation. These two parameters were used to investigate the impact of the crop residue removal rate on the risk of purple soil *P* loss by observing *TP* distribution in aggregates.

This study aimed to investigate the impact of crop residue removal on the erodibility and *P* loss risk in purple soil through an on-farm crop residue removal experiment in purple soil areas. The objectives of this study were (1) to examine the effects of different crop residue removal rates on soil aggregates stability, saturated hydraulic conductivity, and soil erosion risk; (2) to measure the distribution of *TP* in the different sized aggregates of purple soil under different residue removal conditions; and (3) to determine the maximum residue removal rate for the study area.

2. Materials and Methods

2.1. Study Area

In 2018, an on-farm field experiment was conducted in Xinyan Village, Qinglong Town, Jianyang City, Chengdu City, Sichuan Province, China (30°29′11″ N, 104°38′42″ E). The experimental site is located in the hilly region of the Sichuan Basin, with an altitude of 430 m above sea level. The area has a subtropical monsoon climate with abundant rainfall (1190 *mm* annually during the experiment) and high summer temperature (25 °C). Figure 1 shows the monthly rainfall and average monthly temperature during the period when the experiment was conducted. The soil is classified as a Regosol in the Food and Agriculture Organization (FAO) Taxonomy [27], with a purple soil type. A soil sample was collected in April 2018 before the experiment, and the initial soil texture and properties were determined and are presented in Table 1.

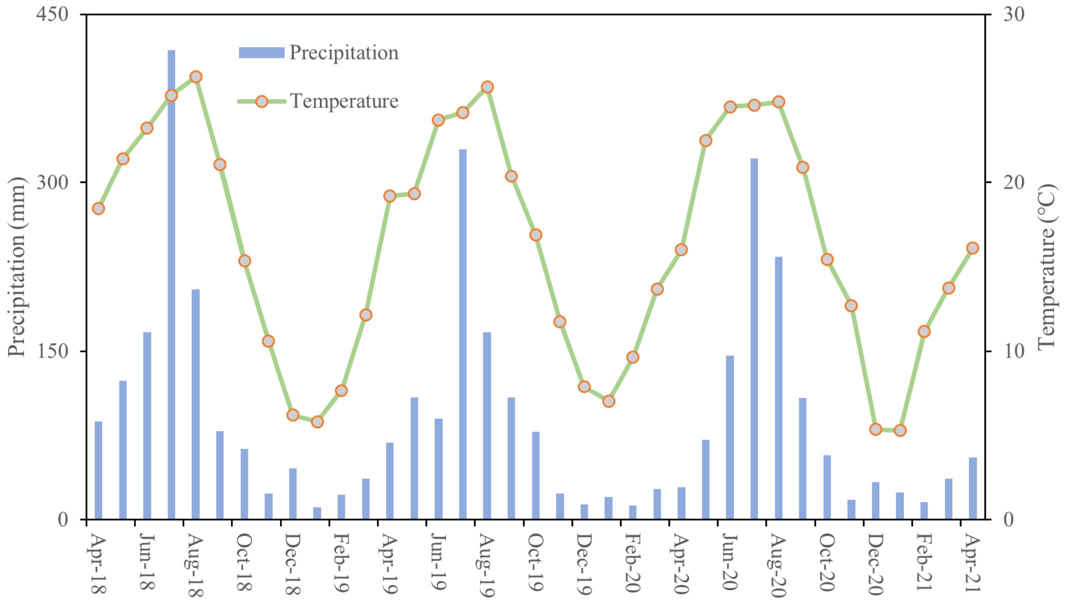

Figure 1. Monthly weather data of Chengdu city (China Meteorlogical Data Network). The bar graph represents the monthly average rainfall, and the line graph represents the monthly average temperature.

Table 1. The soil texture and basic properties of 0–10 cm soil samples.

Texture and Property	Value	Unit
Sand (20–2000 μm)	42	%
Silt (2–20 μm)	26	%
Clay (<2 μm)	32	%
Weight moisture content	18.65	%
Dry density	1.14	$g\ cm^{-3}$
Total N	115	$mg\ g^{-1}$
Total P	420	$mg\ g^{-1}$
SOC	22.07	$mg\ g^{-1}$
IC	29.11	$mg\ g^{-1}$

2.2. Experments Setting

The experiment was conducted in a rotation of summer maize and winter canola on a field with purple soil. Each experimental plot measured 5 × 5 *m*, and the experimental design was a complete randomized block with 3 treatments and 4 replicates. The treatments included crop residue removal at 3 rates (i.e., 0%, 50% and 100% of the total crop straw in the field) after harvest. After each crop was harvested, the corresponding amount of straw was removed at the different removal rates, and the remaining straw was then evenly distributed over the soil surface. Figure 2 shows the experimental field after straw removal at different rates. The study commenced on 29 April 2018 and spanned three years, during which six residue removal treatments were conducted, consisting of three canola straws and three corn straws, as shown in Table 2.

Figure 2. Effects of different crop residue removal rates on field conditions (photographed on 30 April 2020).

Table 2. Soil sampling and residue removal from 29 April 2018 to 8 May 2020.

Texture and Property	Unit
29 April 2018	Initial soil sampling
15 May 2018	Canola residue removal
5 August 2018	Soil sampling
21 August 2018	Maize harvesting
28 August 2018	Maize residue removal
23 April 2019	Soil sampling and canola harvesting
11 May 2019	Canola residue removal
18 August 2019	Maize harvesting
27 August 2019	Maize residue removal
28 April 2020	Soil sampling
30 April 2020	Canola harvesting
1 May 2020	Canola residue removal
20 August 2019	Maize harvesting
23 August 2020	Maize residue removal
29 April 2021	Soil sampling and canola harvesting
8 May 2020	Canola residue removal

Crop residue removal was conducted following local agricultural management practices and the experimental design. After removal, moderate tillage was performed by tumbling and loosening the top 0–10 *cm* of soil. Super phosphate was applied as the main component of the phosphate fertilizer, accounting for more than 12% of $P_2O_5^{2-}$, at a rate of 1500 $kg\ ha^{-1}$ every year. Urea was applied as an N fertilizer at a rate of 825 $kg\ ha^{-1}$ every year. For the summer maize, the phosphate fertilizer was applied twice at rates of 225 $kg\ ha^{-1}$ (fourth week of May every year) and 525 $kg\ ha^{-1}$ (third week of July every year), and urea was applied once at a rate of 450 $kg\ ha^{-1}$ (third week of July every year). For the winter canola, phosphate fertilizer and urea were applied once at the rates of 750 $kg\ ha^{-1}$ and 375 $kg\ ha^{-1}$ (first week of December every year), respectively.

2.3. Soil Sampling

A total of 3 *kg* of soil was randomly sampled from a depth of 0 to 10 *cm* in each research plot. To ensure homogeneity, each soil sample was thoroughly mixed before being allowed to dry naturally. Once dried, any crop residues or other debris were removed from each individual soil sample. The sampling time for each plot is listed in Table 2, and the resulting soil samples were available for physical and chemical property testing.

2.4. Soil Physical Properties

2.4.1. Aggregate Indices Calculation

The fully self-mixed soil samples were passed through a 5–10 *mm* dry sieve, weighed to 50 *g*, and, then, the aggregate particle size classification was performed by the wet sieve method. The samples were placed flat on the top layer of the aggregate analyzer sieve. The apertures of the sieves are 5 *mm*, 2 *mm*, 1 *mm*, 0.5 *mm* and 0.25 *mm* from top to bottom. The soil samples were fully soaked in water by raising the water level high enough to touch the soil particles through capillary action. The stack of sieves was then moved up and down for ten minutes in water to separate the soil aggregates based on size. After wet sieving, soil samples were sorted and collected according to aperture size. Soil aggregates were divided into six categories based on their size ranges: 5–10 *mm*, 2–5 *mm*, 1–2 *mm*, 0.5–1 *mm*, 0.25–0.5 *mm*, and less than 0.25 *mm*. We calculated the mean weight diameter (MWD), geometric mean diameter (GMD), and aggregates with a diameter greater than 0.25 *mm* ($R_{>0.25mm}$) as follows.

$$MWD = \sum_{i=1}^{n} d_i m_i / \sum_{i=1}^{n} m_i \tag{1}$$

$$GMD = Exp\left[\sum_{i=1}^{n} m_i ln d_i / \sum_{i=1}^{n} m_i\right] \tag{2}$$

$$R_{>0.25mm} = \frac{M_{>0.25mm}}{M_T} \tag{3}$$

where d_i indicates the average diameter of aggregates in each size, and m_i represents the proportion of soil aggregate weight in the corresponding size. $M_{>0.25mm}$ refers to the mass of aggregates with a diameter greater than 0.25 *mm*, and M_T is the mass of the sample [28].

2.4.2. Saturated Hydraulic Conductivity

Saturated hydraulic conductivity (k_f) characterizes the infiltration capacity of the soil. In this study, the saturated infiltration coefficient was measured by a Hood Infiltrometer IL-2700 (HI; Umwelt Geräte Technik, GmbH., Shanghai, China www.ugt-online.de (accessed on 25 December 2018)). The instrument works by applying negative pressure over the infiltration zone and injecting water into the infiltrator to bring it to balance within 2–3 h. The stable infiltration rate of the soil surface at different pressures is measured to derive the k_f. The calculation is as follows [31]:

$$k_u = k_f \cdot e^{(\alpha \cdot h)} \tag{4}$$

$$Q = \pi \cdot a^2 \cdot k_u \cdot [1 + 4/(\pi \cdot \alpha \cdot a)] \tag{5}$$

where k_u is the unsaturated permeability coefficient, e is the natural constant, α is the Gardner coefficient, Q is the steady-state flow rate, and a is the radius of the infiltration hood.

2.5. Soil Loss Simulation

The average annual soil erosion modulus, denoted by A ($t\ ha^{-1} a^{-1}$), is a measure of the degree of soil erosion and represents the amount of soil erosion per unit area and unit time [32], In this study, we calculated A using the Revised Universal Soil Loss Equation (2) (RUSLE2), which is described by the following equation [33,34].

$$A = R \cdot K \cdot L \cdot S \cdot C \cdot P \tag{6}$$

where R is the rainfall erosivity factor in ($MJ\ mm\ hm^{-2}\ h^{-1}\ a^{-1}$); R is the soil erodibility factor in ($t\ hm^2\ h\ hm^{-2}\ h^{-1}\ a^{-1}$); LS is the slope length factor (dimensionless); C is the vegetation cover and management factor (dimensionless); P is the soil and water conservation measure factor (dimensionless).

The rainfall erosivity factor, R, represents the potential impact of rainfall and surface runoff on soil erosion. Typically, R is determined based on the daily rainfall in the local area and is calculated using the following equations [35].

$$R = \sum_{m=1}^{24} R_m \tag{7}$$

$$R_m = \alpha \sum_{j=1}^{k} P_j^{\beta} \tag{8}$$

$$\alpha = 21.586\beta^{-7.1891} \tag{9}$$

$$\beta = 0.8363\frac{18.177}{P_{d12}} + \frac{24.455}{P_{y12}} \tag{10}$$

where R_m is the rainfall erosivity ($MJ\ mm\ hm^{-2}\ h^{-1}\ a^{-1}$) in the m-th semimonthly period, k is the number of days in the semimonthly period, P_j is the erosive daily rainfall (mm) on the j-th day in the semimonthly period, α and β are model parameters, P_{d12} is the average daily rainfall (mm) of 12 mm and above, P_{y12} is the average daily rainfall (mm) for daily rainfall of 12 mm and above annual average rainfall (mm). Our average annual rainfall erosion force R was calculated to be 7936.0 $MJ\ mm\ hm^{-2}\ h^{-1}\ a^{-1}$ in the experimental period.

Soil erodibility factor K characterizes comprehensive representation of the soil's ability to resist erosion. In this study, the soil erodibility factor K was calculated by Shirazi's equation as follows [36]:

$$K = 7.594(0.0034 + 0.0405e^{-0.5(\frac{\log(GMD)+1.659}{0.7101})^2}) \tag{11}$$

where GMD is the geometric mean particle size of the soil.

The cultivated land in the Sichuan hilly region typically has a slope ranging from 0 to 15°. To simulate soil erosion, we selected five slopes (0°, 2.5°, 5°, 10°, and 15°). The slope length was set to 5 m i to maintain consistency with the experimental plot size. The LS factor is calculated as follows [37–39]:

$$L = \left(\frac{\lambda}{22.13}\right)^m \tag{12}$$

$$S = \begin{cases} 10.8sin\theta + 0.03,\ \theta < 5^\circ \\ 16.8sin\theta - 0.5,\ 5^\circ \le \theta < 10^\circ \\ 21.91sin\theta - 0.96,\ \theta \ge 10^\circ \end{cases} \tag{13}$$

where λ is the slope length, m is the slope length factor index, and m values are shown in Table 3, and θ is the slope degree.

Table 3. The values of slope length factor index m.

θ	m
$\theta \le 0.5^\circ$	0.2
$0.5^\circ < \theta \le 1.5^\circ$	0.3
$1.5^\circ < \theta \le 2.5^\circ$	0.4
$\theta > 2.5^\circ$	0.5

The C and P factors indicate the influence of mulch management, as well as soil and water conservation practices, on soil erosion. To estimate these factors, a summer maize–

winter canola rotation system was established, with field crop yields for each period and the conversion of maize stover additions at each removal rate. The rotation patterns were then imported into the management submodule of the RUSLE 2 (version 2.6.1.9) model to calculate the C and P factors during the rotation [40].

2.6. Soil Total Phosphorus

2.6.1. TP in the Soil

The soil samples were air-dried, mixed thoroughly, and ground to pass through a 0.149 mm sieve. The TP was determined using the Alkali Fusion–Mo–Sb Anti-spectrophotometric Method [27]. First, the sample was weighed and placed in a nickel crucible, wetted with a few drops of anhydrous ethanol, and, then, sodium hydroxide was added and the sample was laid flat on the surface of the sample. The crucible was then heated in a muffle furnace, and, after it cooled to room temperature, the contents were washed with 3 $mol\ L^{-1}$ sulfuric acid and pure water before being transferred to a centrifuge tube for centrifugation. The supernatant was collected, and the pH was adjusted before adding the color developer. The absorbance was measured at 700 nm with pure water as the reference, and the TP content of the soil sample was obtained by calculation using the following equation.

$$\omega = \frac{[(A - A_0) - a] \times V_1}{b \times m \times \omega_{dm} \times V_2} \tag{14}$$

where A is the absorbance value of the sample, A_0 is the absorbance value of the blank test, a is the intercept of the calibration curve, V_1 is the constant volume of the sample (mL), b is the slope of the calibration curve, m is the mass of the sample (g), ω_{dm} is the dry matter mass fraction of the soil sample, and V_2 is the volume of the test material (mL).

2.6.2. TP in the Aggregates

The soil TP content is influenced by the P content in aggregates of different sizes, and changes in P content in different-sized aggregates can have an impact on the TP content of the soil. Therefore, the soil TP content can be calculated using the flowing equation.

$$C_{TP_{soil}} = \sum_{i=1}^{n} C_{i_{TP}} \times m_i \tag{15}$$

where $C_{i_{TP}}$ is the TP concentration ($mg\ g^{-1}$) of corresponding aggregates, and m_i is the total mass percentage of corresponding aggregates (g).

In Equation (15), the variable m_i is utilized as a weight to calculate the weighted average of the aggregates' TP concentration in order to obtain the $C_{TP_{soil}}$, which represents a mass average value. In the same way, we used m_i as a weight to calculate the geometric weighted average of the aggregates' TP concentration in order to obtain the geometric mean concentration ($GMC_{TP_{soil}}$), which was calculated as follows:

$$GMC_{TP_{soil}} = EXP\left(\frac{\sum_{i=1}^{n} m_i lnC_{i_{TP}}}{\sum_{i=1}^{n} m_i}\right) \tag{16}$$

Based on the Equation (16), we used the particle size diameter of the corresponding aggregates to adjust the weights m_i (while keeping the sum of concentration weights constant) to obtain the geometric mean concentration adjusted by the particle size diameter of the aggregates ($GMC_{TP_{soil}}$), which was calculated as follows:

$$GMC_{dTP_{soil}} = EXP\left(\frac{\sum_{i=1}^{n} m_i \times d_i \times lnC_{i_{TP}}}{\sum_{i=1}^{n} m_i \times d_i}\right) \tag{17}$$

where d_i indicates the average diameter of aggregates in each size, and m_i represents the proportion of soil aggregate weight in the corresponding size.

2.7. Leaching Experiment

To conduct the leaching experiment, a PVC cylinder with an inner diameter of 5 *cm* and a height of 15 *cm* was used as a column. The bottom of the column was covered with a permeable stone layer to prevent soil washout and blockage of the outlet, followed by a 5 *cm* layer of quartz sand. The soil samples were then added uniformly to the column to a height of 10 *cm* and covered with another permeable stone layer to ensure a steady and uniform water flow. After adding 34.2 *mg* of pure potassium dihydrogen phosphate to the top of the soil column, the outlet at the bottom of the sealed soil column was closed. Pure water was passed through the top of the soil column until it was saturated to ensure that the soil column was soaked in pure water for 24 *h*. This ensured that the initial total phosphorus concentration in the soil sample was consistent. In our leaching experiments, the soil columns were soaked before the start of leaching in order to simulate the state of the cultivated land just after the application of fertilizer. In addition, this made it possible to ensure a uniform phosphorus concentration at the start of leaching among soil columns. At this time, merely testing the *TP* concentration in the leaching solution can indicate the impact of different straw removal rates on the risk of phosphorus loss in purple soil. Then, the column was continuously leached for 24 *h* with pure water at a flow rate of 0.42 $mL\ min^{-1}$, and the leachate was collected for *TP* concentration measurement using the Alkali Fusion–Mo–Sb Anti-spectrophotometric Method.

2.8. Statistical Analysis

The experimental data were tested for normality using SPSS (version 26). One-way analysis of variance (ANOVA) was used to determine statistical differences among treatments for soil aggregate fractions, saturated hydraulic conductivity, soil *TP*, and *P* content in each soil aggregate fraction. The differences were compared by least significant difference (LSD), and $p < 0.05$ was considered statistically significant.

3. Results

3.1. Water Stability of Soil Aggregates

3.1.1. Parameters of Wet Sieving

Figure 3 presents the *MWD*, *GMD*, and $R_{>0.25mm}$ of each treatment over time. The *MWD* of different treatments ranged from 1.095 to 2.138 *mm*. In September 2018 and April 2020, the *MWD* under the treatment with 0% residue removal was significantly higher than the other two groups. However, there was no significant difference among the treatment groups in April 2019 and April 2021. Meanwhile, the maximum *MWD* value of all treatment groups appeared in 2019. Among the treatments, the average *MWD* decreased with increasing removal rate (1.809, 1.571, and 1.502 *mm*, respectively). The changing patterns of the *MWD* over time were not obvious in each treatment group.

The difference in the *GMD* between treatments was consistent with that of the *MWD*. In September 2018 and April 2020, the *GMD* under the treatment of 0% residue removal was significantly higher than that of the 50% and 100% removal treatments. Similarly, no significant difference was found in the *GMD* among the treatment groups at other sampling times. The maximum *GMD* values for the 50% and 100% removal treatments appeared one year after the experiment started, but the maximum *GMD* value for the 0% removal treatment appeared two years after the experiment started.

The mass proportion of soil aggregates with diameters > 0.25 *mm* ($R_{>0.25mm}$) in different treatments ranged from 46.30% to 71.92%. In April 2020, the treatment with 0% residue removal significantly increased the proportion of particles with diameters greater than 0.25 *mm* ($R_{>0.25mm}$) compared to the other treatments. However, no clear effect of removal rate on the $R_{>0.25mm}$ was observed at other time points. During the experiment, the treatment with 0% removal rate resulted in an increase and then a decrease in the proportion of particles with a $R_{>0.25mm}$, while the effects of the other two treatments on the $R_{>0.25mm}$ were not significant.

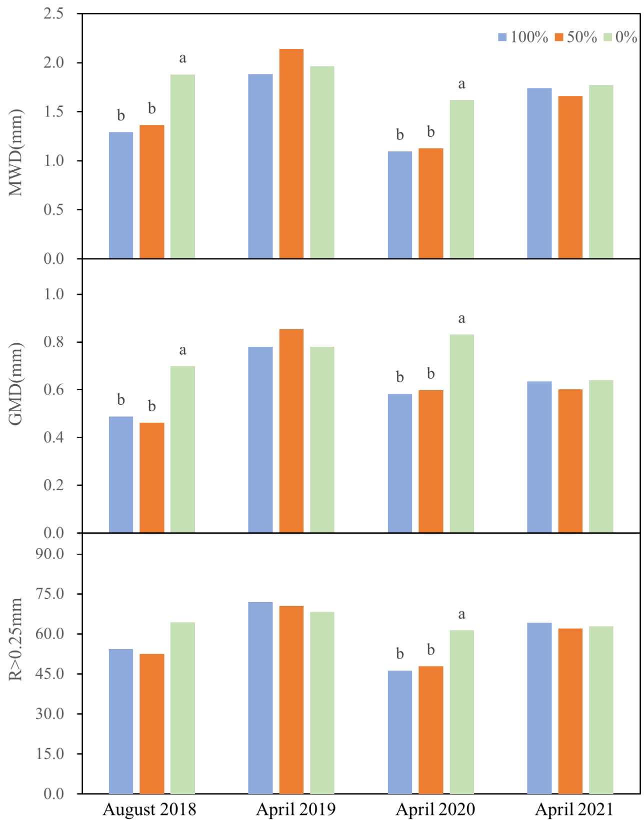

Figure 3. Effects of crop residue removal rates on soil aggregate characteristics. The bars show the distribution of soil aggregates by size, mean weight diameter (*MWD*), geometric mean diameter (*GMD*), and percentage of aggregates larger than 0.25 mm ($R_{>0.25mm}$). The lowercase letters indicate significant differences among treatments within each sampling period ($p < 0.05$). No letters indicate no significant differences. The numbers 0%, 50%, and 100% represent the crop residue removal rates for each treatment.

3.1.2. Mass Distribution of Soil Aggregates

Table 4 presents the mass proportion of soil aggregate in different sizes. After 4 months of experiments, compared with other treatments, the percentage of 2–5 *mm* aggregates was significantly increased with the full crop residue retention. After one year of experiments, the proportion of 1–2 *mm* aggregates in the complete residue removed treatment was significantly higher than the other two treatments. After two years of experiments, the proportion of 0.25–0.5 *mm* aggregates was significantly reduced in the 100% removal treatment, while the proportion of <0.25 *mm* aggregates was significantly reduced in the 0% removal treatment. However, after three years of experiment, no significant differences were found in the distribution of different aggregates among the different residue removal treatments. The response of different aggregates sizes to treatments and the mass percentages of the aggregates with the same sizes did not differ consistently across years.

Table 4. Mass percentages of aggregates in different sizes during August 2018 to April 2021.

Time	Removal	Soil Aggregate Soil Particle Size					
		>5 mm	2–5 mm	1–2 mm	0.5–1 mm	0.25–0.5 mm	<0.25 mm
August 2018	100%	6.27	14.09 b	8.54	12.75	12.69	45.67
	50%	7.59	14.07 b	7.60	10.80	12.47	47.47
	0%	11.47	19.84 a	10.18	11.73	11.13	35.65

Table 4. *Cont.*

Time	Removal	Soil Aggregate Soil Particle Size					
		>5 mm	**2–5 mm**	**1–2 mm**	**0.5–1 mm**	**0.25–0.5 mm**	**<0.25 mm**
April 2019	100%	10.97	19.05	12.23 a	16.93	12.74	28.08
	50%	15.25	18.65	10.22 b	14.23	12.03	29.63
	0%	17.99	19.33	11.35 b	14.03	10.25	27.05
April 2020	100%	3.39	11.77	6.65	13.68	10.82 b	53.70 a
	50%	4.55	11.24	5.85	10.15	16.03 a	52.20 a
	0%	4.32	12.61	10.52	18.31	15.54 a	38.70 b
April 2021	100%	11.18	16.27	8.71	13.81	14.20	35.83
	50%	10.09	16.14	9.21	13.53	13.09	37.95
	0%	11.46	16.54	9.50	13.15	12.15	37.21

The lowercase letters above the bars indicate significant differences among treatments at the same sampling period.

3.1.3. Saturated Hydraulic Conductivity

The effect of different straw removal rate treatments on the saturated hydraulic conductivity of the soil was measured after one year since the experiment initiated, and the results are presented in Figure 4. The greatest coefficient k_f of 79.44 $mm\ min^{-1}$ was measured in the 100% removal treatment, whereas the lowest soil saturated infiltration coefficient of 7.32 $mm\ min^{-1}$ was recorded in the complete removal treatment. The coefficient k_f of the soil without straw removal (0% straw removal treatment) was significantly higher than the other two treatments, and it even reached 2.56 times higher than that of the soil subjected to full residue removal (100% straw removal treatment).

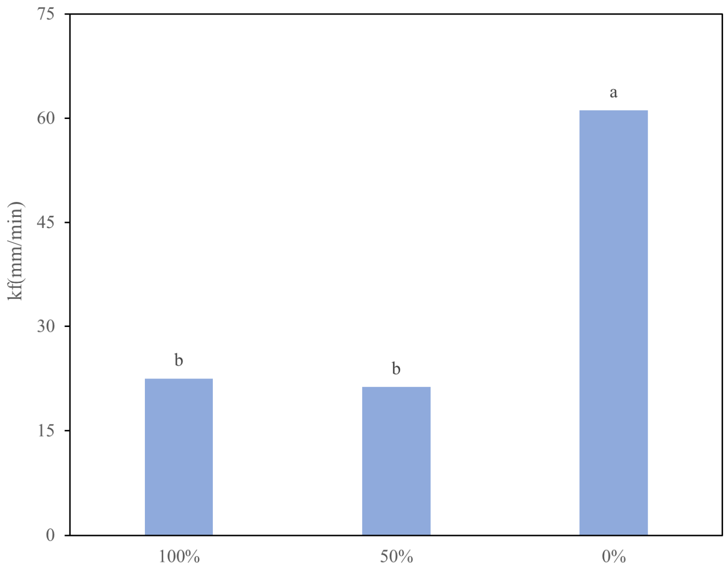

Figure 4. Effects of crop residue removal rates on soil saturation permeability. The bars show the mean values and the lowercase letters indicate significant differences among treatments ($p < 0.05$). The numbers 0%, 50%, and 100% represent the crop residue removal rates for each treatment.

3.2. RUSLE 2

Figure 5 depicts the impact of three different crop residue removal rates on the soil erosion modulus A at various land slope conditions. The retention of straw on farmland as a low-cost agronomic technique effectively improves soil's resistance to erosion. However, cropland with steep slopes is always at a high risk of erosion, regardless of straw retention. At 0° slope, partial or complete straw retention resulted in relatively low soil loss. At a 2.5° slope, the soil loss remained low under different residue removal rates, with the 0% removal treatment resulting in only 12.00 $t\ ha^{-1}\ a^{-1}$ of soil loss. However, at a 5° slope, complete straw removal resulted in soil losses of over 150 $t\ ha^{-1}\ a^{-1}$. As the cultivated land slope increased to 10°, soil losses significantly increased for all treatments, with increases of 124.1%, 129.3%, and 129.6% compared to the 5° slope for the 100%, 50%, and 0% removal treatments, respectively. At a slope of 15°, except for the 0% removal treatment, the soil loss for the other two treatments exceeded 200 $t\ ha^{-1}\ a^{-1}$. The effect of lower crop residue removal rates on soil erosion loss gradually decreased with an increase in slope. The soil loss for the complete removal treatment was 33.2 times higher at a 15° slope than at a 0° slope; the 50% removal treatment was 107.5 times higher at a 15° slope than at a 0° slope; and the 0% removal treatment was 245.5 times higher at a 15° slope than at a 0° slope. Overall, straw retention was effective in reducing the risk of soil erosion.

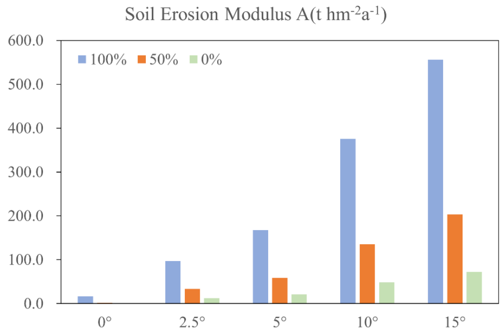

Figure 5. Effects of crop residue removal rates and land slope on soil erosion modulus A ($t\ ha^{-1}\ a^{-1}$). The bars show the mean values for each treatment. The numbers 0%, 50%, and 100% represent the crop residue removal rates for each treatment. Significant differences were observed among all treatments within each land slope ($p < 0.05$).

3.3. TP Content

3.3.1. Soil TP Concentration

Figure 6 shows the result of the soil *TP* concentrations under different crop residue removal rates over the years. The results indicate that overall, straw removal did not significantly affect the soil *TP* concentration over the course of the experiment, except in 2019. Soil *TP* concentrations for the 100%, 50%, and 0% straw removal rate treatments were 0.615–1.005 $g\ kg^{-1}$, 0.695–1.232 $g\ kg^{-1}$, and 0.517–1.000 $g\ kg^{-1}$ respectively, in different durations of treatment. The soil *TP* concentration of 1.232 $g\ kg^{-1}$ was highest in the 50% straw removal rate treatment in 2019. In comparison to the 2018 soil *TP* concentrations, only the 100% straw removal rate treatment soil *TP* concentration changed significantly (increased) in 2021. Compared with the 100% straw removal rate treatment, the 50% straw removal rate treatment increased soil *TP* concentration in 2019 by 35.6%.

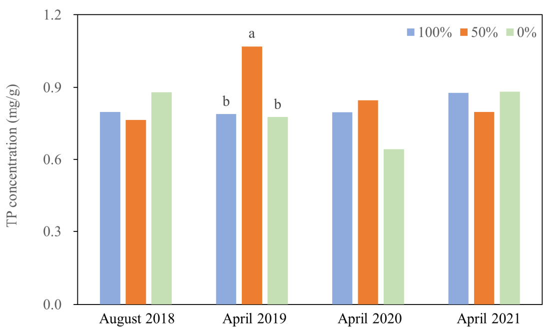

Figure 6. Effects of crop residue removal rates on *TP* concentration. Different lowercase letters above the bars indicate significant differences among treatments ($p < 0.05$). No letters indicate no significant difference. The treatments are 0%, 50%, and 100% crop residue removal rates.

3.3.2. TP Content Percentage of Aggregates

Figure 7 presents the soil *TP* content percentages in different aggregate size fractions of each treatment over time. Not removing crop residue can lead to a greater enrichment of *P* in larger aggregates. The highest soil *TP* content percentage of aggregates < 0.25 *mm* in size was observed in three treatments at all four sampling periods, while no significant differences were found among the treatments at each sampling period. After four months of experimentation (August 2018), the treatment with 0% straw removal resulted in a significantly higher percentage of *TP* content in the 2–5 *mm* aggregates compared to the other two treatments. Removing 100% of the straw compared to retaining it significantly increased the percentage of *TP* content in smaller aggregates (0.5–1 *mm* and 0.25–0.5 *mm*). After one year of experimentation (April 2019), different residue removal rates mainly affected the *TP* content percentage in the 0.25–1 *mm* aggregates. However, unlike the observation results in September 2018, complete straw removal did not result in a higher enrichment of *P* in the 0.25–0.5 *mm* aggregates. The 0% removal treatment resulted in a significantly higher percentage of *TP* content in the 0.5–1 *mm* aggregates compared to the other treatments. In contrast, the 50% removal treatment resulted in a significantly higher percentage of *TP* content in the 0.25–0.5 *mm* aggregates compared to the other treatments. Conversely, the 100% straw removal rate treatment resulted in a significantly higher percentage of *TP* content in the medium-sized aggregates (1–2 *mm*) compared to the treatment with retained straw. After two years of experimentation (April 2020), the 0% straw removal rate treatment resulted in a significantly higher percentage of *TP* content in the 1–2 *mm* aggregates compared to the other treatments. After three years of experimentation (April 2021), similar to the results in August 2018, retaining all the straw helped distribute more *P* to larger aggregates (2–5 *mm*), with the 0% straw removal rate treatment being significantly higher than the complete removal rate treatment by 28.43%.

Figure 7. Percentage of *TP* content of aggregates in different sizes in response to different residue removal rates. The treatments are 0%, 50%, and 100% crop residue removal rates.

3.4. *GMC* and GMC_d

The Figure 8 shows the *GMC* and GMC_d values for each treatment during the entire experiment. The *GMC* values for the 100% and 0% residue removal treatments both exhibited a trend of first decreasing and then increasing, with the minimum values for both treatments occurring after one year (0.731 $g\ kg^{-1}$) and two years (0.613 $g\ kg^{-1}$) of the experiment, respectively. In contrast to the other two treatments, the trend for the *GMC* value for the 50% straw removal treatment was first increasing and then decreasing, with the maximum value occurring after one year of the experiment (0.985 $g\ kg^{-1}$). In April 2019, the *GMC* value for the 50% straw removal treatment was significantly higher than that for the 100% and 0% straw removal treatments (by 25.7% and 23.1%, respectively).

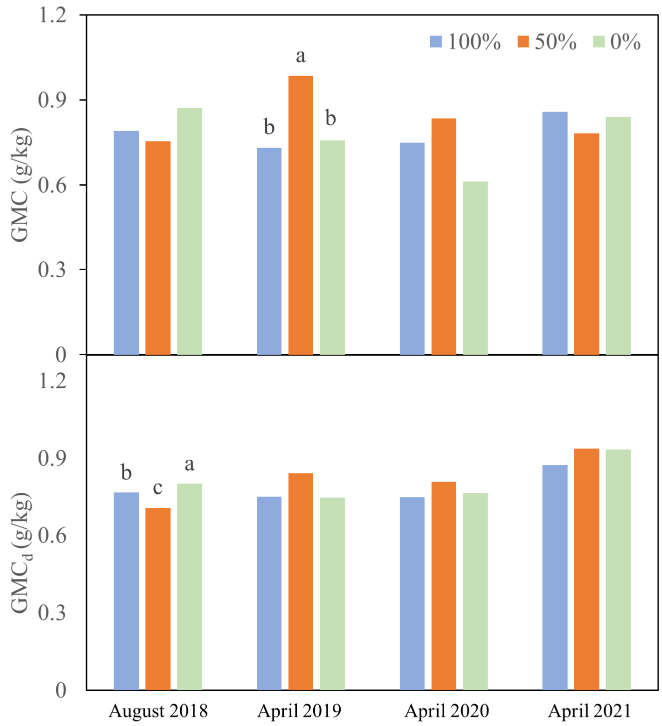

Figure 8. *GMC* and GMC_d values under different residue removal rates. Different lowercase letters above the bars indicate significant differences among treatments ($p < 0.05$).

After four months of the experiment, there was a significant difference in GMC_d values among the three treatments, with the order of GMC_d values from high to low being 0%, 100%, and 50% removal treatments, respectively. However, in subsequent sampling periods, there was no significant difference in GMC_d among treatments with different residue removal rates. Compared with the complete removal treatment, the 50% and 0% removal treatments showed a larger increase in GMC_d (compared with the data from August 2018) in April 2021, with increases of 14.3%, 32.7%, and 16.6% for the 100%, 50%, and 0% residue removal treatments, respectively.

3.5. TP Concentration of Leaching Liquid

Figure 9 shows the changes in the *TP* concentration of leachate from different treatments during the leaching experiment. The *TP* concentration in the leachate from the 50% and 0% straw removal treatments was consistently lower than that from the complete straw removal treatment. Furthermore, the *TP* concentration in the leachate increased with an increase in straw removal rate, but the trends in the changes in *TP* concentration in the leachate for the three treatments were different. The *TP* concentration in the leachate for the 0% removal treatment gradually increased, the rate of increase in the *TP* concentration in the leachate for the 50% removal treatment was lower than that for the 0% removal treatment, and the *TP* concentration in the leachate from the 100% straw removal treatment showed a trend of initially increasing and then decreasing. Compared with the other two treatments, long-term and continuous full crop residue retention in the field led to a gradual weakening in the degree of reduction in the *TP* concentration in the leachate.

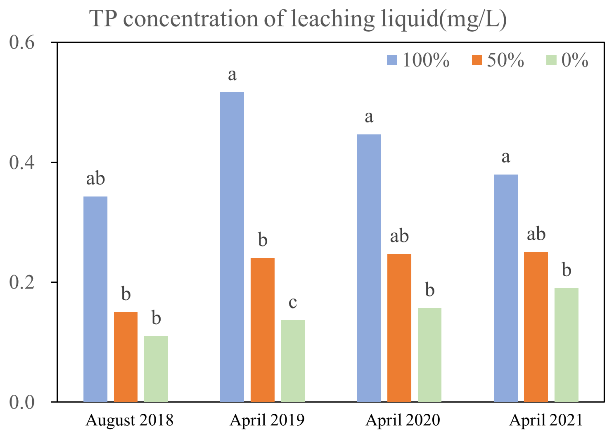

Figure 9. *TP* concentration of leachate under different residue removal rates. Different lowercase letters above the bars indicate significant differences among treatments ($p < 0.05$).

4. Discussion

4.1. Impact of Crop Residue on Soil Aggregate Distribution and Stability

Soil aggregate composition is influenced by a variety of factors [41], including dynamic interactions between the organic matter contained in the soil and its various mineral components. Key indicators of soil aggregate particle size distribution include the $R_{>0.25mm}$, *MWD*, and *GMD*, with higher values typically indicating a lower potential for soil erosion. Purple soils are characterized by low organic matter content and poor soil structure, which increase the risk of soil erosion [42]. Our study revealed that the retention of all crop residue in the field led to an improvement in soil aggregate stability, along with an increase in the proportion of larger aggregates, which is in line with the findings reported by Zhang et al. [43]. The incorporation of crop straw into the soil was observed to promote the aggregation of soil particles, thereby resulting in the formation of more stable aggregates. This enhancement in aggregate stability was attributed as the primary factor for the observed increase in the proportion of larger aggregates. However, we did not consistently observe the same results over the course of the three-year study, and we attribute this to the disruption of soil aggregate structure due to the short period between soil sampling and tillage. As shown in Table 2, soil sampling was conducted on the same day as crop harvest in both April 2019 and April 2021. However, it should be noted that soil sampling after crop harvest is likely to have a significant impact on the distribution of topsoil [44], which may have contributed to the inconsistency in aggregate stability observed in our study.

Soil saturation permeability is a measure of the ease with which water can penetrate the soil. A lower permeability coefficient indicates higher surface runoff and stronger erosive effects on the soil [45]. In our study, we observed that the infiltration coefficient of the soil with 0% crop residue removal treatment was significantly higher than that of the soils where partial or all residue was removed. This is consistent with Ibrahim, Vahyala E et al. [46], who suggest that retaining crop residue can improve soil permeability, reduce surface runoff, and decrease the risk of soil erosion. Based on our findings, we recommend that crop residue removal operations in purple soil regions should not remove crop residue in order to maintain soil aggregate stability.

4.2. Impact of Crop Residue on Soil Erosion

Soil erosion has been a major threat to agricultural productivity [47]. Our experimental findings (Figure 5 simulation of soil erosion modulus A) demonstrate a significant increase in soil erosion with increasing crop residue removal rates. Crop straw covering the soil surface directly reduces the impact of raindrops on the soil and decreases water flow by increasing the roughness of the soil surface. Thus, residue removal leads to more significant soil erosion due to the impact of raindrops on the soil and increased surface runoff [48]. Notably, although retaining straw in the field helps to reduce soil erosion, steep-sloped farmland (with slopes over 2.5°) still poses a high risk for sustainable agriculture, even with crop residue retention.

Purple soils in the southwestern hilly region of China are characterized by high weathering and low water and fertilizer retention capacity. In terms of erosion, these soils are ranked just below yellow soils among agricultural production soils, and returning straw to the soil is considered an effective management measure for reducing soil erosion [49]. Studies [27] indicated that annual topsoil erosion should not exceed 11.04 $t\ ha^{-1}\ a^{-1}$ to maintain safe agricultural production. Based on the results of the RUSLE 2 simulation, it was found that the soil erosion of 50% and 0% straw removal treatments only met the minimum criteria for maintaining the productivity and fertility of purple soils at a slope of 0°. Moreover, the effect of retaining residue on mitigating soil erosion risk was weaker on sloping arable land than on less sloping arable land. Previous studies [27,50] on purple soil erosion also indicated that purple soil had lower erosion resistance than other soils, and even a slight slope would greatly increase the erosion risk. The RUSLE 2 model simulation results showed that purple soils have a higher erosion risk and that an increase in soil loss would also result in an increase in *P* loss with the soil. Therefore, to achieve sustainable agricultural development and reduce non-point source pollution in purple soil cultivated land, it is recommended not to remove crop residues in purple soil regions, and land leveling should be carried out simultaneously.

4.3. Impact of Straw on TP of Aggregates

When simulating *P* loss through leaching experiments, we found a significant decrease in *TP* concentration in the leachate when crop residue was retained compared to its complete removal. However, regardless of the straw removal rate, the *TP* concentration in the leachate was lower than 5 $mg\ L^{-1}$, thus indicating a low risk of loss. This finding is consistent with the results reported by Liu Jin et al. [51], wherein different cover management can have an impact on the risk of phosphorus loss, but the *TP* concentration in the leaching solution remains at a low level. Although retaining crop residues for an extended period does not result in a continued reduction in the loss of soluble *P*, the risk of dissolved *P* loss remains lower compared to the treatment where all residues are removed.

Aggregates serve as the fundamental building blocks of soil structure and play a pivotal role in the storage and stabilization of soil *P* [52]. Klopp Hans W et al. [53] found that straw takes a very long time to mineralize and does not release *P* well to replenish the soil. Furthermore, studies have demonstrated that the binding of *P* to crop residue diminishes the anchoring of *P* in the soil [51]. In our experiment, no clear pattern of change in soil *P* was observed under different crop residue removal treatments. When the influence of straw removal on soil *P* loss risk could not be directly obtained from soil *TP* concentration and *TP* distribution in aggregates, we proposed two parameters, the *GMC* and GMC_d, to represent the distribution of *TP* in aggregates and to assess whether *P* was more enriched in larger aggregates. We believed that a greater enrichment of *P* in larger aggregates, as compared to smaller aggregates, could effectively mitigate the risk of soil *P* loss. There is no universal theory that can fully explain the sequence of erosion of soil particles based on their size. However, it is generally observed that smaller particles are more susceptible to erosion than larger ones. Therefore, in order to more accurately reflect the distribution of *P* in soil particles, we adjusted the geometric mean concentration of the *TP* by incorporating the mass of aggregates. The calculation method is as follows:

$$GMC = \sqrt[\sum_1^n m_i]{\prod_1^n C_i{}^{m_i}} \tag{18}$$

This formula can be simplified as Equation (16). We adjusted the *GMC* using aggregate size and introduced the parameter d_i/d_0 inside the GMC_d to account for the weight of the *TP* in different aggregates. The calculation is derived as follows:

$$GMC_d = \sqrt[\sum_1^n \frac{d_i}{d_0} * m_i]{\prod_1^n C_i^{\frac{d_i}{d_0} * m_i}} \tag{19}$$

where d_i is the particle size of the corresponding aggregate, and d_0 represents a value of the average particle size, which can be combined with di in the form of d_i/d_0 as a dimensionless constant value for calculation. This equation can be simplified as Equation (17) (d_i can be dispensed with in the final expression and does not need to be calculated).

The preceding paragraphs describe the derivation process of *GMC* and GMC_d. In contrast to the traditional method of expressing *TP* concentration, we included the distribution of *P* in soil aggregates of different particle sizes and adjusted the soil *TP* concentration accordingly. Ultimately, we used the GMC_d value to assess the risk of soil *P* loss. Assuming that two soil samples, A and B, have identical total *P* concentrations, if the *P* distribution in sample A is skewed toward larger aggregates, and the *P* distribution in sample B is skewed toward smaller aggregates, then the *P* loss risk in sample A is lower than in sample B. This is because larger aggregates possess stronger erosion resistance than smaller ones, thus providing better retention of *P* in larger aggregates during soil erosion. Hence, assessing the risk of *P* loss in soil solely based on the *TP* concentration is not adequate. Formula (19) indicates that, as the aggregate size increases, the GMC_d value also increases. Therefore, the GMC_d value can be used to determine *P* distribution in aggregates, where a higher GMC_d corresponds to more *P* being distributed in larger aggregates. Since multiple studies on the effect of straw on soil *P* loss risk have not reached a consensus, it is essential to supplement multiple indicators, such as the *GMC* and GMC_d, to examine the impact of straw on soil *P* loss risk.

Unfortunately, our experiment did not reveal any significant changes in the GMC_d among the different residue removal treatments. We attribute this to the fertilization treatment being conducted too close to the sampling time, which greatly influenced the observation results. Furthermore, the three-year duration of the straw removal treatment may not be sufficient to observe changes in *P* loss risk in agricultural production. Our experimental findings suggest that retaining straw facilitates *P* to be more evenly distributed in larger aggregates. Although straw cannot directly impact the soil's *P* content, it can sequester more *P* in the soil's stable aggregates, which lowers the risk of soil *P* loss.

5. Conclusions

In order to promote sustainable agricultural development in the purple soil region of southwestern China, we investigated the impact of crop residue removal on soil aggregate stability, soil erosion risk, and *P* loss risk in purple soil aggregates. A three-year on-farm experiment was conducted to analyze the distribution of soil aggregates, saturated hydraulic conductivity, soil erosion, *P* distribution, and *P* loss under different residue removal levels. The main conclusions are as follows: (1) the *GMC* and GMC_d can serve as indicators for evaluating *P* distribution in soil aggregates and can be used to assess soil *P* loss risk. (2) Complete and partial crop residue removal can damage soil aggregate structure, increase soil erosion loss, and reduce the retention of soil *P* in large aggregates, which can lead to higher risks of soil erosion and *P* loss in purple soils. Therefore, residue removal practices are not recommended in the purple soil region. (3) More experimental data should be collected to verify the feasibility of using the *GMC* and GMC_d as indicators for *P* loss risk assessment.

Author Contributions: Methodology, K.Y. and Y.H.; software, C.Z., M.L. and K.Y.; validation, Y.H., K.Y. and W.Z.; formal analysis, K.Y.; investigation, C.L.; resources, Y.H. and W.Z.; data curation, K.Y.; writing—original draft preparation, K.Y.; writing—review and editing, Y.H.; supervision, L.L.; project administration, Y.H.; funding acquisition, Y.H. All authors have read and agreed to the published version of the manuscript.

Funding: This research was funded by the Major Science and Technology Projects of Sichuan Province, grant number 2023YFN0067; the National Natural Science Foundation of China, grant number 51709190; and the Sichuan Science and Technology Program, grant number 2022YFS0472.

Conflicts of Interest: The authors declare that they have no known competing financial interests or personal relationships that could have appeared to influence the work reported in this paper.

References

1. Zhu, B.; Wang, T.; You, X.; Gao, M.-R. Nutrient release from weathering of purplish rocks in the Sichuan Basin, China. *Pedosphere* **2008**, *18*, 257–264. [CrossRef]
2. He, X.; Zheng, Z.; Li, T.; He, S.; Zhang, X.; Wang, Y.; Huang, H.; Yu, H.; Liu, T.; Lin, C. Transport of colloidal phosphorus in runoff and sediment on sloping farmland in the purple soil area of south-western China. *Environ. Sci. Pollut. Res.* **2019**, *26*, 24088–24098. [CrossRef] [PubMed]
3. Lin, C.; Tu, S.; Huang, J.; Chen, Y. The effect of plant hedgerows on the spatial distribution of soil erosion and soil fertility on sloping farmland in the purple-soil area of China. *Soil Tillage Res.* **2009**, *105*, 307–312. [CrossRef]
4. Zhong, S.; Han, Z.; Duo, J.; Ci, E.; Ni, J.; Xie, D.; Wei, C. Relationships between the lithology of purple rocks and the pedogenesis of purple soils in the Sichuan Basin, China. *Sci. Rep.* **2019**, *9*, 13272. [CrossRef]
5. Guo, Z.L.; Zhong, C.; Cai, C.F.; Ding, S.W.; Wang, Z.M. Nitrogen competition in contour hedgerow systems in subtropical China. *Nutr. Cycl. Agroecosyst.* **2008**, *81*, 71–83. [CrossRef]
6. Fang, Y.R.; Wu, Y.; Xie, G.H. Crop residue utilizations and potential for bioethanol production in China. *Renew. Sustain. Energy Rev.* **2019**, *113*, 109288. [CrossRef]
7. Yin, H.; Zhao, W.; Li, T.; Cheng, X.; Liu, Q. Balancing straw returning and chemical fertilizers in China: Role of straw nutrient resources. *Renew. Sustain. Energy Rev.* **2018**, *81*, 2695–2702. [CrossRef]
8. Liu, J.G.; Diamond, J. China's environment in a globalizing world. *Nature* **2005**, *435*, 1179–1186. [CrossRef]
9. Bhattacharyya, P.; Chakraborty, A.; Bhattacharya, B.; Chakrabarti, K. Evaluation of MSW compost as a component of integrated nutrient management in wetland rice. *Compos. Sci. Util.* **2003**, *11*, 343–350. [CrossRef]
10. Korsaeth, A.; Eltun, R. Nitrogen mass balances in conventional, integrated and ecological cropping systems and the relationship between balance calculations and nitrogen runoff in an 8-year field experiment in Norway. *Agric. Ecosyst. Environ.* **2000**, *79*, 199–214. [CrossRef]
11. Vitousek, P.M.; Naylor, R.; Crews, T.; David, M.B.; Drinkwater, L.E.; Holland, E.; Johnes, P.J.; Katzenberger, J.; Martinelli, L.A.; Matson, P.A.; et al. Nutrient Imbalances in Agricultural Development. *Science* **2009**, *324*, 1519–1520. [CrossRef] [PubMed]
12. Dalzell, B.J.; Johnson, J.M.F.; Tallaksen, J.; Allan, D.L.; Barbour, N.W. Simulated Impacts of Crop Residue Removal and Tillage on Soil Organic Matter Maintenance. *Soil Sci. Soc. Am. J.* **2013**, *77*, 1349–1356. [CrossRef]
13. Riedell, W.E.; Osborne, S.L.; Dagel, K.J. Maize Residue Removal and Cover Crop Effects on Subsequent Soybean Crops. *Agron. J.* **2017**, *109*, 2762–2770. [CrossRef]
14. Ding, X.; Xue, Y.; Lin, M.; Liu, Y. Effects of Precipitation and Topography on Total Phosphorus Loss from Purple Soil. *Water* **2017**, *9*, 315. [CrossRef]
15. Wei, O.; Cai, G.-Q.; Huang, H.-B.; Geng, X.-J. Temporal-spatial distribution of agricultural diffuse nitrogen pollution and relationship with soil respiration and nitrification. *Huan Jing Ke Xue* **2014**, *35*, 2411–2418.
16. Guo, Z.; Liu, H.; Hua, K.; Wang, D.; He, C. Long-term straw incorporation benefits the elevation of soil phosphorus availability and use efficiency in the agroecosystem. *Span. J. Agric. Res.* **2018**, *16*, e1101. [CrossRef]
17. Fu, B.; Chen, L.; Huang, H.; Qu, P.; Wei, Z. Impacts of crop residues on soil health: A review. *Environ. Pollut. Bioavailab.* **2021**, *33*, 164–173. [CrossRef]
18. Sims, J.T.; Edwards, A.C.; Schoumans, O.F.; Simard, R.R. Integrating soil phosphorus testing into environmentally based agricultural management practices. *J. Environ. Qual.* **2000**, *29*, 60–71. [CrossRef]
19. Bos, J.; Williams, M.; Smith, D.; Armstrong, S.; Harmel, D. Long-term effect of poultry litter application on phosphorus balances and runoff losses. *J. Environ. Qual.* **2021**, *50*, 639–652. [CrossRef]
20. Lin, C.; Defu, L.; Linxu, S.; Yujie, C.; Ge, Z. Research on nutrient export mechanism of runoff from yellow-brown soil slopes under different rain intensity. *Environ. Sci.* **2013**, *34*, 2151–2158. (In Chinese) [CrossRef]
21. Lin, C.; Linxu, S.; Yujie, C.; Biao, Z.; Xiaoming, Z.; Defu, L. Research on phosphorus loss patterns in yellow-brown soil slopes under simulated rainfall conditions. *J. Agro-Environ. Sci.* **2013**, *32*, 49–55. (In Chinese)
22. Sims, J.T. Phosphorus soil testing: Innovations for water quality protection. *Commun. Soil Sci. Plant Anal.* **1998**, *29*, 1471–1489. [CrossRef]
23. Szerlag, K.D.; Elavarthi, M.; Siebecker, M.G.; Gu, C.; McCrone, C.; Sparks, D.L. Systematic Study of Legacy Phosphorus (P) Desorption Mechanisms in High-P Agricultural Soils. *Minerals* **2022**, *12*, 458. [CrossRef]
24. Chen, M.; Li, Y.; Wang, C.; Walter, T. An investigation of the effects of humic acid on soil erosion and loss of phosphorus from soil to runoff: Experiment and modeling. *Geoderma* **2022**, *427*, 116121. [CrossRef]
25. Dunkerley, D. The case for increased validation of rainfall simulation as a tool for researching runoff, soil erosion, and related processes. *Catena* **2021**, *202*, 105283. [CrossRef]

26. Wang, J.; Wang, D.; Zhang, G.; Wang, Y.; Wang, C.; Teng, Y.; Christie, P. Nitrogen and phosphorus leaching losses from intensively managed paddy fields with straw retention. *Agric. Water Manag.* **2014**, *141*, 66–73. [CrossRef]
27. Zhang, P.; He, Y.; Ren, T.; Wang, Y.; Liu, C.; Li, N.; Li, L. The Crop Residue Removal Threshold Ensures Sustainable Agriculture in the Purple Soil Region of Sichuan, China. *Sustainability* **2021**, *13*, 3799. [CrossRef]
28. Cao, D.; Lan, Y.; Sun, Q.; Yang, X.; Chen, W.; Meng, J.; Wang, D.; Li, N. Maize straw and its biochar affect phosphorus distribution in soil aggregates and are beneficial for improving phosphorus availability along the soil profile. *Eur. J. Soil Sci.* **2021**, *72*, 2165–2179. [CrossRef]
29. Li, Y.; Wang, J.; Shao, M.a. Earthworm inoculation and straw return decrease the phosphorus adsorption capacity of soils in the Loess region, China. *J. Environ. Manag.* **2022**, *312*, 114921. [CrossRef]
30. Wang, S.L.; Liu, Y.H.; Song, X.L.; Wei, S.B.; Li, J.P.; Nie, J.J.; Qin, D.L.; Sun, X.Z. Effects of cotton straw returning on soil organic carbon, nitrogen, phosphorus and potas-sium contents in soil aggregates. *Ying Yong Sheng Tai Xue Bao* **2016**, *27*, 3944–3952. [CrossRef]
31. Matula, S.; Mihalikova, M.; Lufinkova, J.; Batkova, K. The role of the initial soil water content in the determination of unsaturated soil hydraulic conductivity using a tension infiltrometer. *Plant Soil Environ.* **2015**, *61*, 515–521. [CrossRef]
32. Kinnell, P.I.A. Event soil loss, runoff and the Universal Soil Loss Equation family of models: A review. *J. Hydrol.* **2010**, *385*, 384–397. [CrossRef]
33. Wischmeier, W.H. Relation of Field-Plot Runoff to Management and Physical Factors. *Soil Sci. Soc. Am. Proc.* **1966**, *30*, 272–277. [CrossRef]
34. Wischmeier, W.H.; Mannering, J.V. Relation of Soil Properties to Its Erodibility. *Soil Sci. Soc. Am. Proc.* **1969**, *33*, 131–137. [CrossRef]
35. Wenbo, Z.; Yun, X.; Baoyuan, L. Rainfall Erosivity Estimation Using Daily Rainfall Amounts. *Sci. Geogr. Sin.* **2002**, *22*, 705–711. [CrossRef]
36. Shirazi, M.A.; Boersma, L. A Unifying Quantitative-Analysis of Soil Texture. *Soil Sci. Soc. Am. J.* **1984**, *48*, 142–147. [CrossRef]
37. Liu, B.Y.; Nearing, M.A.; Risse, L.M. Slope Gradient Effects on Soil Loss for Steep Slopes. *Trans. Asae* **1994**, *37*, 1835–1840. [CrossRef]
38. McCool, D.K. Effects of Slope Length and Steepness on Soil-Erosion from Rangelands. In *Proceedings of the Workshop on Estimating Erosion and Sediment Yield on Rangelands, Tucson, Arizona, 7–9 March 1981*; U.S. Department of Agriculture: Washington, DC, USA, 1982; pp. 73–95.
39. Wischmeier, W.H. The Usle—Some Reflections. *J. Soil Water Conserv.* **1984**, *39*, 105–107.
40. Li, P.; Zang, Y.; Ma, D.; Yao, W.; Holden, J.; Irvine, B.; Zhao, G. Soil erosion rates assessed by RUSLE and PESERA for a Chinese Loess Plateau catchment under land-cover changes. *Earth Surf. Process. Landf.* **2020**, *45*, 707–722. [CrossRef]
41. Voltoini, M.; Tas, N.; Wang, S.; Brodie, E.L.; Ajo-Franklin, J.B. Quantitative characterization of soil micro-aggregates: New opportunities from sub-micron resolution synchrotron X-ray microtomography. *Geoderma* **2017**, *305*, 382–393. [CrossRef]
42. Xia, R.; Shi, D.; Ni, S.; Wang, R.; Zhang, J.; Song, G. Effects of soil erosion and soil amendment on soil aggregate stability in the cultivated-layer of sloping farmland in the Three Gorges Reservoir area. *Soil Tillage Res.* **2022**, *223*, 105447. [CrossRef]
43. Zhang, P.; Wei, T.; Jia, Z.; Han, Q.; Ren, X. Soil aggregate and crop yield changes with different rates of straw incorporation in semiarid areas of northwest China. *Geoderma* **2014**, *230*, 41–49. [CrossRef]
44. Olson, K.R.; Al-Kaisi, M.M. The importance of soil sampling depth for accurate account of soil organic carbon sequestration, storage, retention and loss. *Catena* **2015**, *125*, 33–37. [CrossRef]
45. Miller, J.J.; Owen, M.L.; Yang, X.M.; Drury, C.F.; Chanasyk, D.S.; Willms, W.D. Water Repellency and Hydrophobicity of Some Major Agricultural Crop Residues. *Agron. J.* **2019**, *111*, 3008–3019, Erratum in *Agron. J.* **2020**, *112*, 1474. [CrossRef]
46. Ibrahim, V.E.; Osborne, S.L.; Schumacher, T.E.; Riedell, W.E. Corn Residue Removal Effects on Hydraulically Effective Macropores. *Commun. Soil Sci. Plant Anal.* **2018**, *49*, 1491–1501. [CrossRef]
47. Kavian, A.; Gholami, L.; Mohammadi, M.; Spalevic, V.; Falah Soraki, M. Impact of Wheat Residue on Soil Erosion Processes. *Not. Bot. Horti Agrobot. Cluj-Napoca* **2018**, *46*, 553–562. [CrossRef]
48. Zhao, X.; Liu, S.-L.; Pu, C.; Zhang, X.-Q.; Xue, J.-F.; Ren, Y.-X.; Zhao, X.-L.; Chen, F.; Lal, R.; Zhang, H.-L. Crop yields under no-till farming in China: A meta-analysis. *Eur. J. Agron.* **2017**, *84*, 67–75. [CrossRef]
49. Khan, M.N.; Gong, Y.; Hu, T.; Lal, R.; Zheng, J.; Justine, M.F.; Azhar, M.; Che, M.; Zhang, H. Effect of Slope, Rainfall Intensity and Mulch on Erosion and Infiltration under Simulated Rain on Purple Soil of South-Western Sichuan Province, China. *Water* **2016**, *8*, 528. [CrossRef]
50. Luo, B.; Han, Z.; Yang, J.; Wang, Q. Assessment of Erosion Characteristics in Purple and Yellow Soils Using Simulated Rainfall Experiments. *Int. J. Environ. Res. Public Health* **2022**, *19*, 357. [CrossRef]
51. Liu, J.; Sui, P.; Cade-Menun, B.J.; Hu, Y.; Yang, J.; Huang, S.; Ma, Y. Molecular-level understanding of phosphorus transformation with long-term phosphorus addition and depletion in an alkaline soil. *Geoderma* **2019**, *353*, 116–124. [CrossRef]
52. Ranatunga, T.D.; Reddy, S.S.; Taylor, R.W. Phosphorus distribution in soil aggregate size fractions in a poultry litter applied soil and potential environmental impacts. *Geoderma* **2013**, *192*, 446–452. [CrossRef]
53. Klopp, H.W.; Blanco-Canqui, H. Implications of crop residue removal on soil physical properties: A review. *Soil Sci. Soc. Am. J.* **2022**, *86*, 979–1001. [CrossRef]